Enhanced Active Sulfur in Soft Carbon via Synergistic Doping Effect for Ultra–stable Lithium–ion Batteries

Bing Sun[a], Qin Zhang[a,*], Hui Xiang[a], Fei Han[b], Wen Tang[a], Guanming Yuan[a], Ye Cong[a], Changling Fan[b], Aidan Westwood[c], Xuanke Li[a, b, **]

[a] The State Key Laboratory of Refractories and Metallurgy, Wuhan University of Science and Technology, Wuhan 430081, China

[b] Hunan Province Key Laboratory for Advanced Carbon Materials and Applied Technology, Hunan University, Changsha 410082, China

[c] School of Chemical and Process Engineering, University of Leeds, Leeds, LS2 9JT, United Kingdom

[*]Corresponding author. E–mail addresses: zhangqin627@wust.edu.cn (Q. Zhang);
[**]Corresponding author. E–mail addresses: xkli8524@sina.com (X.K. Li).

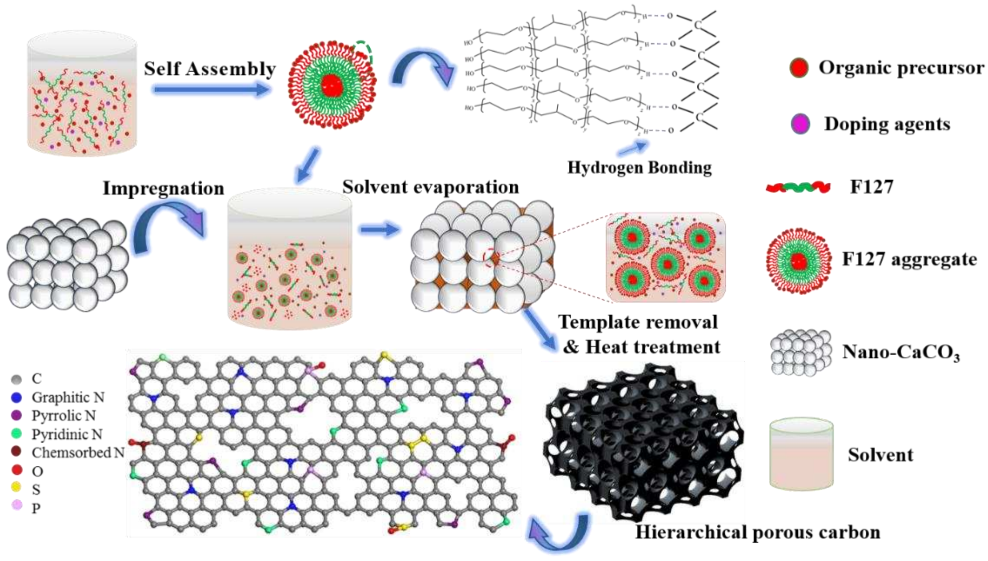

Fig. S1. Schematic illustration of preparation process of heteroatoms doped hierarchical porous carbon framework.

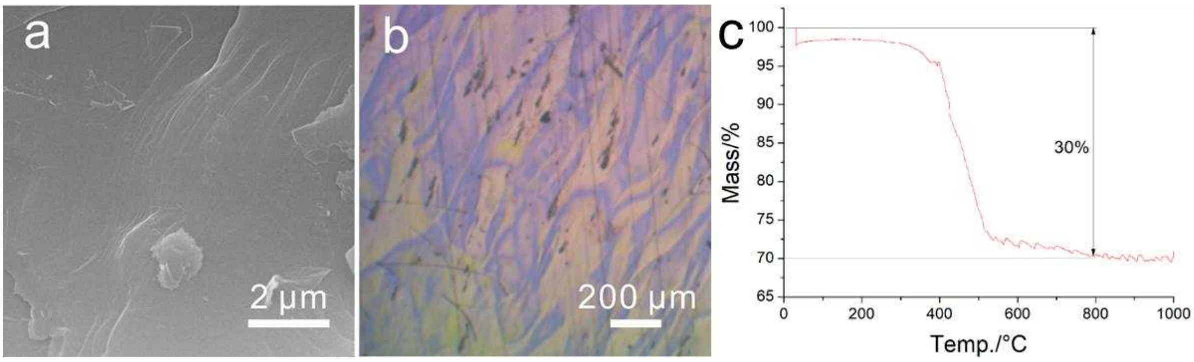

Fig. S2. (a) SEM of the carbon without templates and dopants, (b) Optical micrograph of the raw material of mesophase pitch and (c) TG curve of MP at N_2 atmosphere.

Table S1. Typical properties of MP.

Mesophase content	Softening point (℃)	Hydrogen/Carbon	Ash (ppm)
100%	275–295	0.58–0.64	<20

Table S2. Elemental analysis of MP.

C (at%)	H (at%)	S (at%)	H/C
95.13	4.89	0.15	0.61

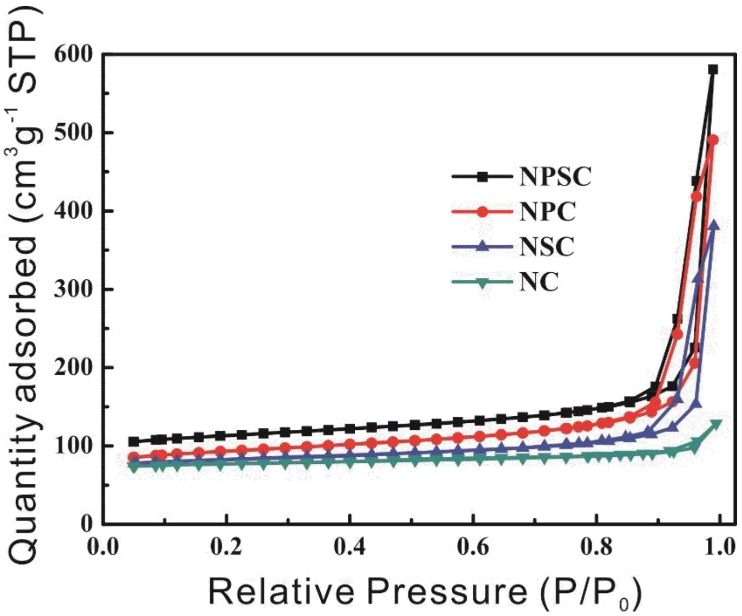

Fig. S3. Nitrogen adsorption/desorption isotherms.

Table S3. Specific surface areas and pore parameters of samples.

Sample	Surface area (m^2/g)	Pore volume (cm^3/g)
NC	113.5	0.20
NSC	125.8	0.26
NPC	132.7	0.31
NPSC	163.1	0.43

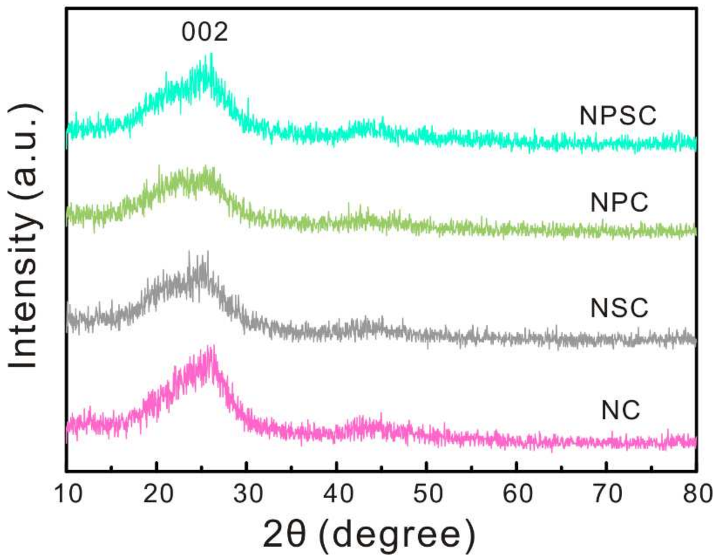

Fig. S4. XRD of NC, NSC, NPC and NPSC.

Table S4. Bulk compositions of the prepared materials obtained from the EA results.

	EA [a]				**Doping concentration** [b]		
	C	**N**	**H**	**S**	**N/C**	**H/C**	**S/C**
NC	83.81	8.36	1.26	-	8.55	1.80	-
NSC	77.01	7.89	1.21	2.62	8.78	1.89	1.27
NPC	76.14	7.64	0.87	-	8.60	1.37	-
NPSC	74.64	5.50	1.23	3.65	6.32	1.97	1.83

[a] wt.%

[b] atomic ratio ×100 (%)

Table S5. Surface compositions of the prepared materials obtained from the XPS analysis.

	C[a]	O[a]	N[a]	S[a]	P[a]	N/C[b]	S/C[b]	P/C[b]
NC	78.72	11.56	9.71	-	-	12.33	-	-
NSC	76.77	11.48	10.78	0.8	-	14.04	1.04	
NPC	81.82	8.67	8.85	-	0.84	10.81	-	1.03
NPSC	75.32	13.41	9.6	0.95	0.65	12.75	1.26	0.86

[a] at%

[b] atomic ratio ×100 (%)

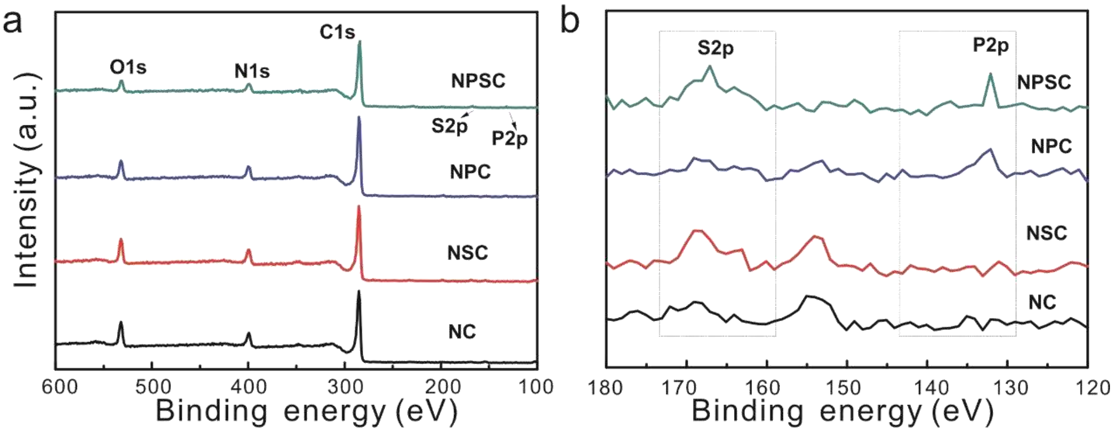

Fig. S5. (a) XPS survey spectra and (b) magnification of NC, NSC, NPC and NPSC.

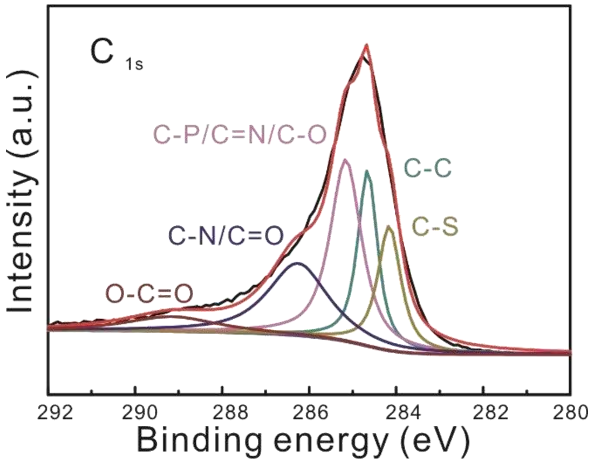

Fig. S6. High-resolution XPS spectra of C 1s for NPSC.

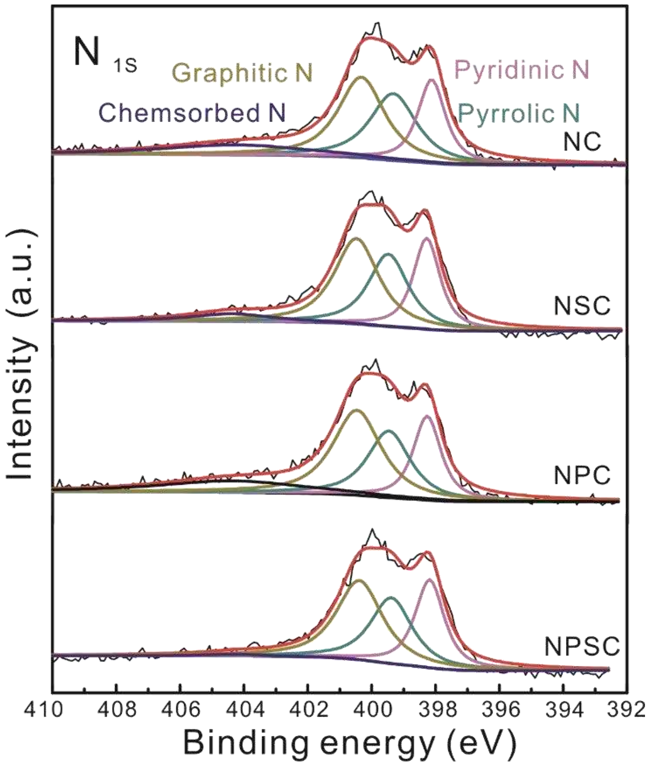

Fig. S7. The XPS results are deconvoluted with pyridinic–N, graphitic–N, pyrrolic–N and pyridinic oxide for XPS–N1s.

Table S6. Various doping types and their fractions for N, S, and P at the carbon surface.

	N-doping (%)[a]				S-doping (%)[b]		P-doping (%)[c]		
	N_1	N_2	N_3	N_4	S_1	S_2	P_1	P_2	P_3
NC	21.89	29.28	35.04	13.79	-	-	-	-	-
NSC	26.35	27.94	37.50	8.20	12.44	87.56	-	-	-
NPC	25.07	29.64	38.97	6.32	-	-	89.67	-	10.33
NPSC	28.43	30.23	40.26	1.08	53.26	46.74	57.21	36.23	6.56

[a] N_1 (Pyridinic-N; 398.6 eV), N_2 (Pyrrolic-N; 399.4 eV), N_3 (Graphitic-N; 400.4 eV), and N_4 (Pyridinic oxide; 402-404 eV);

[b] S_1 (sulphide C-S-C/S-P), and S_2 (sulphone C-SO_x-C);

[c] P_1 (P-C; 132.7 eV), P_2 (P-S; 133.8 eV) and P_3 (P-O; 134-136 eV).

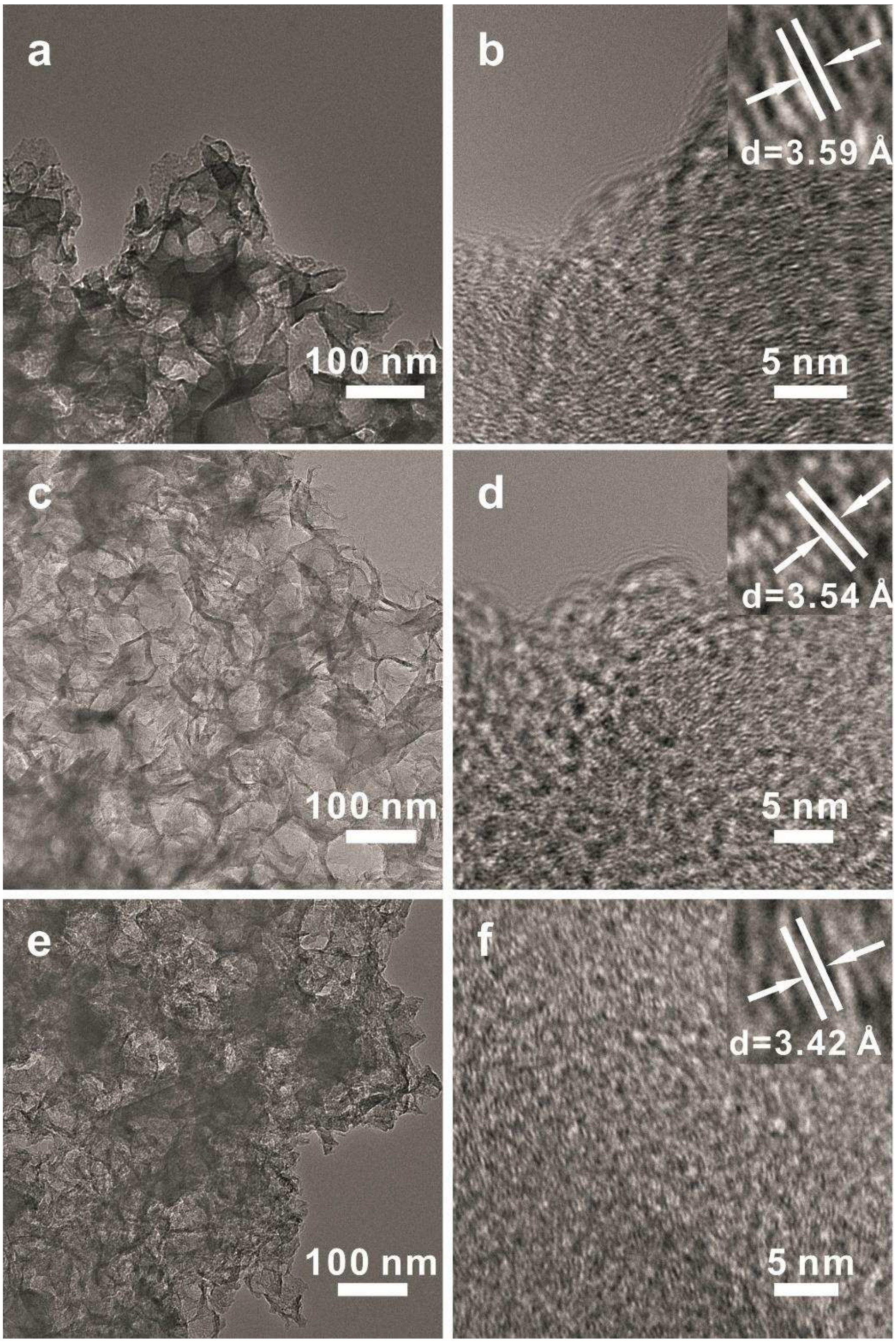

Fig. S8. TEM images of (a, b) NPC; (c, d) NSC; (e, f) NC.

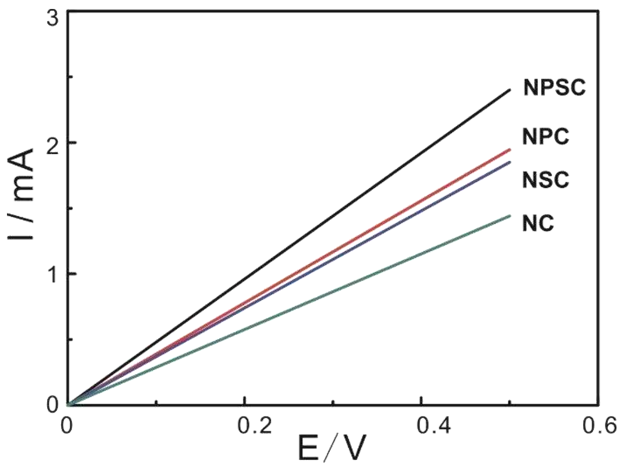

Fig. S9. I-V curves of the wafers containing the as-prepared porous carbon materials.

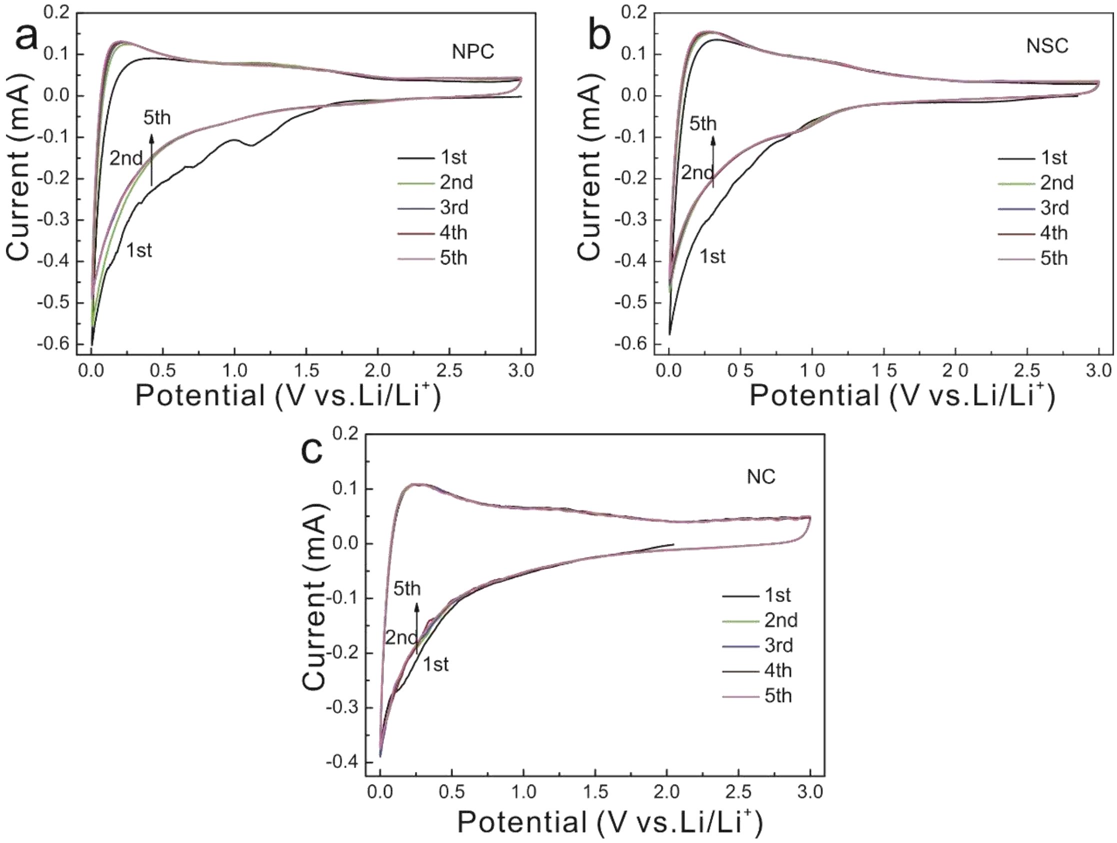

Fig. S10. The voltammetry of the (a) NPC, (b) NSC and (c) NC in the first five cycles between 0.05 and 3.00 V at 0.1 mV s^{-1}.

Table S7. Results of electrochemical performance tests of all samples.

Sample	1^{st} charge capacity (mAh g^{-1})	1^{st} discharge capacity (mAh g^{-1})	1^{st} irreversible capacity (mAh g^{-1})	100^{th} discharge capacity (mAh g^{-1})	1^{st} Coulombic efficiency (%)
NC	872.0	462.4	409.6	346.9	53.03
NSC	900.5	529.7	370.8	481.1	58.82
NPC	946.6	545.1	401.5	508.7	57.58
NPSC	1239.8	770.0	537.2	650.0	62.10

Table S8. Comparison of the electrochemical performance of NPSC with those of reported carbonaceous materials in LIBs.

Sample	Current densities	Reversible capacity	Cyclic performance	Reference
NPSC	100 mA/g	770 mAh/g	Capacity of 650 mAh/g at 100 mA/g over 100 cycles and 510 mAh/g at 500 mA/g over 500 cycles	This work
Pitch-based carbon	0.1C	360 mA h/g	Capacity of 280 mAh/g at 2 C over 100 cycles	[1]
3DGNW	0.1 C	497 mAh/g	Capacity of 297 mAh/g at 1 C over 1000 cycles	[2]
N-doped GPC	100 mA/g	551 mAh/g	Capacity of 328 mAh/g at 0.5 A over 100 cycles	[3]
P-doped soft carbon	0.1C	452 mAh/g	Capacity of 319 mAh/g at 0.5 C over 50 cycles	[4]
P-doped soft carbon	0.2 C	467 mAh/g	Capacity of 379 mAh/g at 1 C over 50 cycles	[5]

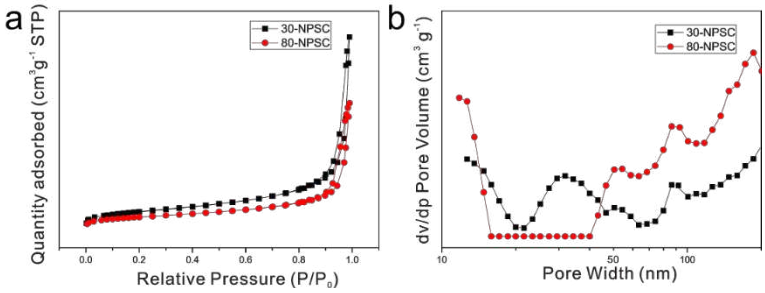

Fig. S11. The Nitrogen adsorption–desorption isotherm curve (a) and pore size distribution (b) of the obtained 30–NPSC and 80–NPSC.

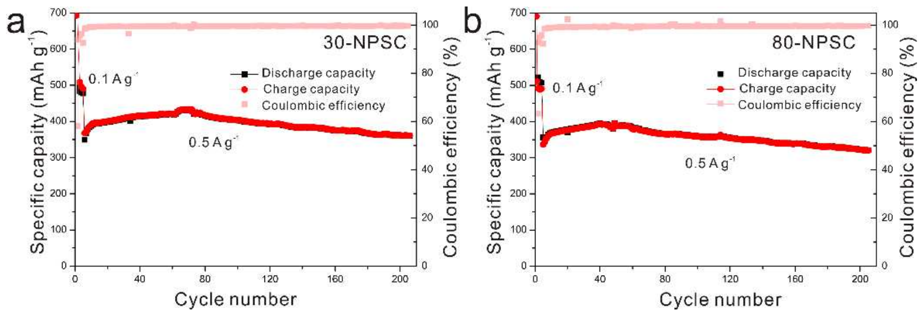

Fig. S12. Long cycling performance of 30–NPSC (a) and 80–NPSC (b) at 0.5 A g^{-1}.

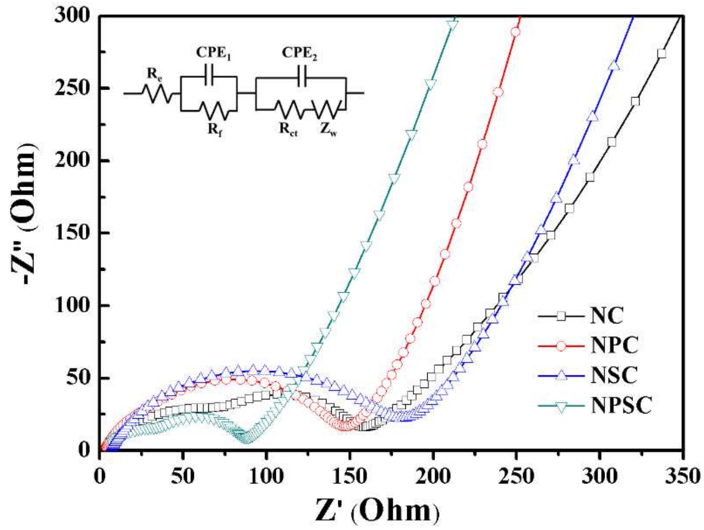

Fig. S13. Nyquist plot of NPSC, NPC, NSC and NC electrodes after 100 cycles and an equivalent circuit inset of it.

Table S9. The typical fitted parameters in the electrochemical impedance spectroscopy.

Sample	NC	NSC	NPC	NPSC
R_e (Ω)	15.63	11.37	10.89	7.63
R_f (Ω)	46.64	52.96	34.24	20.17
R_{ct} (Ω)	66.29	76.68	63.61	50.86

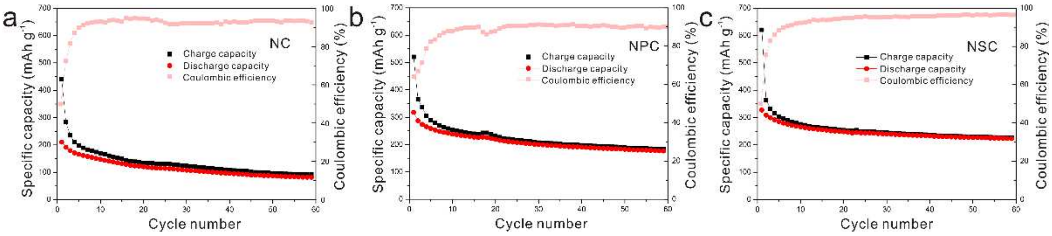

Fig. S14. The cycling stability of full cells with NC (a), NPC (b) and NSC (c) as anodes.

References

[1] F. Sun, J. Gao, Y. Yang, Y. Zhu, L. Wang, X. Pi, X. Liu, Z. Qu, S. Wu, Y. Qin, Carbon 109 (2016) 747-754.

[2] A.L.M. Reddy, A. Srivastava, S.R. Gowda, H. Gullapalli, M. Dubey, P.M. Ajayan, ACS Nano 4 (2010) 6337-6342.

[3] Q. Liang, Y. Zheng, C. Du, Y. Luo, J. Zhang, B. Li, Y. Zong, Q. Yan, Small Methods 1 (2017) 1700304.

[4] E.H. Kim, Y. Jung, Carbon Lett. 15 (2014) 277-281.

[5] M.J. Kim, J.T. Yeon, K. Hong, S.I. Lee, N.S. Choi, S.S. Kim, B. Korean Chem. Soc. 34 (2013) 2029-2035.